Scientific Journal for Damietta Faculty of Science **15**(2) 2025, 237-246
Doi: 10.21608/sjdfs.2025.389541.1234
ISSN Print 2314-8594
ISSN Online 2314-8616

https://sjdfs.journals.ekb.eg/

Structural, Thermal and Transport Properties of 1,2,9-trimethyl-7*H*-furo[3,2-*f*]chromen-7-one]

A. M. Melad[*1,2], N. A. El- Ghamaz[1] and M. M. El-Shabaan[1]

[1]Department of Physics, Faculty of Science, Damietta University, Damietta 34517, Egypt.
[2]Department of Physics, Faculty of Education, Alzintan University, AL zintan, Libya.

Received: 27 May 2025 /Accepted: 01 July 2025

[*]Corresponding author's E-mail: 00afaf.ali00@gmail.com

Abstract

A coumarine derivative namely1,2,9-trimethyl-7*H*-furo[3,2-*f*]chromen-7-one] (TFC) is subjected to investigate thermal, structural, and AC conduction properties. The XRD investigation showed that TFC in powder form is polycrystalline and demonstrates monoclinic crystal system. Thermo-grave metric analyses proved that TFC has a good thermal stability from room temperature up to approximately 460 K. furthermore, it undergoes decomposition in one major step in the temperature range 460 – 583 K. Ac and dc electrical conductivity measurements revealed that TFC showed a semiconductor behavior. The thermal activation energy for DC conductivity ΔE_{dc} are found to be 0.0576 and 0.617 eV in the low and high temperature regions, respectively. The analyses of AC conductivity as a function of temperature and frequency revealed that the correlated barriers hoping (CBH) conduction mechanism is the dominant mechanism for conduction of charge carriers in TFC. The related parameters for the CBH are calculated.

Keywords: Coumarine, XRD, thermal properties, AC conductivity, electrical modulus, Correlated barrier hopping (CBH)

Introduction

Among organic materials is Coumarin family which is naturally occurring organic compound. Coumarin derivatives are utilized in various fields like medicine, dyes, and fluorescence (P n.d.; Sontisiri et al. 2025; Sun et al. 2020). Coumarin was first isolated in 1820 (Sarker and Nahar 2017). Coumarin and its derivatives have gained considerable attention for decades because of their wide range of applications in Pharmacology (Barot et al. 2015; Kadhum et al. 2011; Xu et al. 2021) and biological activity (Mohammed and Ahamed 2022).

Researches continue to produce new coumarin derivatives and providing insights into how modifications can enhance their functionality and effectiveness in biological systems (Detsi, Kontogiorgis, and Hadjipavlou-Litina 2017). Also, the change of substituent group certainly will affect thermal properties of coumarins. This effect appeared obviously in the

derivatives of 2-[(4-Methyl-2-oxo-2H-chromen-7-yl)oxy]-N'-(substitutedmethylene) where the milting point is varied from 252ºC to 298ºC (Satyanarayana et al. 2009). Many coumarin derivatives showed photoluminescence and electroluminescence properties (Kotchapadist et al. 2015; Pramod, Renuka, and Nadaf 2019). The presence of these properties strongly recommend caumarin derivatives in optoelectronic application such as OLEDs (Goel et al. 2012; Kumar, Puttaraju, and Patil 2016). Also, some coumarin derivatives have been investigated as temperature thermometer in polymer-supported materials (Pedro et al. 2023).

Kotchapadist et al. reported that, N-Coumarin derivatives demonstrated thermal stability up to a temperature of about 400 ºC and recommended these derivatives for OLED due to the precast of emission spectra in the visible region of spectra. The emission properties of these N-Coumarin derivatives have been tuned by varying thiophene units in the conjugated backbone or changing the type of substituent (Kotchapadist et al. 2015).

To our knowledge, there is no direct investigation concerning the ac conductivity properties of natural or synthetic Coumarins. In this study we aimed to extract infarction about the thermal stability of new synthesized coumarine derivative as well as its structural and electrical properties arriving to the possible conduction mechanisms, which can help in propose these compounds under investigation for the suitable technological applications.

Experimental

Materials

In the present study, one of the coumarine derivatives which is 1,2,9-trimethyl-7*H*-furo[3,2-*f*]chromen-7-one] (TFC) (Elgogary, Hashem, and Khodeir 2015) is subjected to investigation without any further treatment. The chemical structure of TFC shown in Fig.1.

Thermal Analysis

Thermo gravimetric analysis (TGA) and differential scanning calorimetric (DSC) measurements are recorded by (Simultaneous Thermal Analyzers DSC/TGA, TA Instruments STD Q600) in the temperature range 300 - 650 K. `

X-ray Diffraction Analysis

The crystal structure of TFC in powder form is investigated by using X-Ray diffraction (XRD) technique and recorded by "D2 phaser company bruker, Germany" X-ray diffractometer having Cu as a target. The Ni-filtered CuK_{α} radiation of wavelength (λ= 1.5406 Å) is used. The X-ray tube's voltage and current were 30 kV and 10 mA, respectively. The experimental results are analyses using fullprof software (Dinnebier n.d.; Lin et al. 2008), and optimized by Chekcell software (Tan and Shaari 2008).

Alternating current (AC) measurements

The AC measurements are carried out by the programmable automatic RLC bridge model Hioki 3532-50 LCR Hi Tester, in the frequency range from 100 Hz to 1 MHz and temperature range 300 - 443 K. The powder of TFC is compressed to form pellets under a pressure of 5 tons/cm^2. The resulting pellets have a diameter of 1.2 cm and a thickness of about 1 mm. The samples are placed in a holder specially designed to minimize stray capacitance. The temperature of the sample is monitored during the measurements by using a NiCr-NiAl thermocouple. All measurements are done in dark and in air.

Results and Discussion

Thermal

The TGA and DTG curves for TFC, in the temperature rang 300 – 650 K are presented in Figs.2 and 3.The carves prove a good thermal stability from room temperature up to approximately 460 K. It is noticed that TFC is undergo decomposition in one major step in the temperature range 460 – 583 K with a maxima transition temperature of 581 K (see Fig.3).
Fig.4 presents the DSC charts of TFC in the temperature range 300 – 650 K. It is found that, the first endothermic peaks for TFC is in the range 473 – 492 K. Taking into account that, there is no loss of mass occurs up to this temperatures range, it can be confirmed that all these endothermic peaks can be attributed to the melting process at melting temperature (T_m). The values of T_m can be extracted from DSC

curve and found to be about 500K. This result is confirmed by visual observation by melting apparatus. The last endothermic peaks in the DSC curves for TFC is positioned at the same temperature of this maximum transition temperature which extracted from DTG (see Fig 3). Taking this observation into account, the phase transition process at temperature 585 TFC can be attributed to boiling process at boiling temperature (T_b). As a conclusion, and TFC is thermally stable up to the 500 K. This result recommend the suitable temperature range of studying the dielectric properties and conductivity to be in the range from room temperature to temperature below the melting temperature (T_m). At this point, it is worth to replace the expiration "decomposition" in TGA analyses at the temperature range 555-581 K with the term "loss of mass by evaporation due to boiling process".

X-ray diffraction (XRD)

The XRD patterns of TFC in the diffraction angle range 2θ = 4 -70º is illustrated in Fig.5. The XRD pattern is characterized by many sharp peaks which confirm the polycrystalline nature of TFC in the powder form. Crystal structure system, lattice parameters and Miller indices (*hkl*) of the investigated compounds are obtained by fullprof software (Dinnebier n.d.; Lin et al. 2008), and optimized by Chekcell software (Tan and Shaari 2008). It is found that the TFC has monoclinic crystal system with optimized space group $P1_2/m$ All mentioned parameters are computed and summarized in Tables 1 and 2.

The average crystallite size *D* can be calculated using the following well known Scherre's equation(El-Ghamaz, Moqbel, and El-Shabaan 2020):

$$D = \frac{m\lambda}{\beta_{hkl}\,COS\theta_{hk}}, \quad (1)$$

where $\beta_{hkl.}$ Is the full width at half maximum in radians, λ is the wavelength of the incident x-ray (λ=1.5406 *Å*) and θ_{hkl} the diffraction angle of the peak with miller indices *hkl*. Also the dislocation density δ and the micro strain μ can be calculated using the following relations (Correlation between ionic radii of metal azodye complexes and electrical conductivity n.d.; El-Nahass et al. 2008)

$$\delta = \frac{1}{D^2} \quad (2)$$

$$\mu = \frac{\beta_{hkl}\,COS\theta_{hkl}}{4} \quad (3)$$

The values of *D,* δ and μ is calculated and listed in Table 3.

Dielectric properties

Electrical Modulus

The dielectric modulus $\widetilde{M}$ defined as the inverse of the complex permittivity $\tilde{\varepsilon}$ and is a concept used in the study of dielectric materials practically in analyzing relaxation processes and conductivity. The complex dielectric constant $\tilde{\varepsilon}$ can be expressed by the following relation (Conducting Polymers. VII. Effect of Doping with Iodine on the Dielectrical and Electrical Conduction Properties of Polyaniline n.d.):

$$\tilde{\varepsilon} = \varepsilon_1 - i\varepsilon_2 \quad (4)$$

where ε_1 is the real part and ε_2 is the imaginary part of the dielectric constant. ε_1 and ε_2 are calculated by using the following relations (Dielectrical properties and conduction mechanism of quinoline Schiff base and its complexes n.d.; El-Nahass and Ali 2012):

$$\varepsilon_1 = c\frac{d}{\varepsilon_0 A} \quad (5)$$

$$\varepsilon_2 = \varepsilon_1 tan\delta \quad (6)$$

where ε_o is the permittivity of the free space, *C* is the measured capacitance and *tanδ* is the measured dissipation factor of the three compound in the tablet form. Also, the complex electric modulus, $\widetilde{M}$ given by the following relation (Jung 2013):

$$\widetilde{M} = M_1 + i\,M_2 \quad (7)$$

where M_1 and M_2 are the real and imaginary parts of the electric modulus respectively, and can be calculated from the dielectric constant using the following relations (El-Nahass and Ali 2012):

$$M_1 = \frac{\varepsilon_1}{\varepsilon_1^2+\varepsilon_2^2} \quad (8)$$

$$M_2 = \frac{\varepsilon_2}{\varepsilon_1^2+\varepsilon_2^2} \quad (9)$$

The obtained values of M_1 and M_2 for TFC as a function of frequency are depicted in Figs. 6 and ٧, respectively. In the low frequency region, the values of M_1 tends to zero. This behavior suggests that the compound TFC exhibit minimal polarization or motion at these frequencies. This behavior is typical in materials that may not have yet reached their

characteristic response times which are needed to effectively transition through energy states(Barsoukov and Macdonald 2005). The more increase of test frequency, the more increase of M_1 as seen in Fig. 6. This behavior could be due to the enhancement of polarization of the TFC, as higher frequencies enable more active molecular dynamics and dipole orientations contributing to the overall dielectric response(Liu, Cole, and Low 2013). The spectra of M_1 demonstrate a peak around 1000 Hz which is shifted toward higher frequency with increasing temperature. It is often attributed to thermal activation of charge carriers,(Bose and Sarma n.d.). As temperature rises, molecular motion increases, allowing the materials to respond to oscillating electric fields with higher frequency, thus shifting the peak to higher frequencies (Jonscher 1999).

Fig.7 shows the variation of M_2 with frequency for TFC. It is noticed that, a typical relaxation peak that moves towards higher frequencies by increasing temperature. The presence of a typical relaxation peak indicates that the materials exhibit a relaxation process that is sensitive to frequency. As temperature increases, this peak shifts towards higher frequencies, suggesting that the molecular dynamics become faster at elevated temperatures (El-Ghamaz, Moqbel, and El-Shabaan 2020; Yu et al. 2017). The characteristic relaxation time is calculated by inverse of frequency of the maximum position, i.e., $\tau=1/f_{max}$. The variation of τ with temperature of TFC is calculated and depicted in Fig.7. It is clear that the behavior of relaxation time is affected by the temperature and shows decreasing trend in general and has a peak value at about 348 K (El-Nahass, El-Barry, and Abd el Rahman 2006; Jung 2013; Yu et al. 2017).

Electrical conductivity

The AC (alternating current) electrical conductivity is critically important in material science. It provides insight into the behavior and properties of material especially under alternating electric field and give information about how charge carriers move through a material. The AC electrical conductivity (σ_{ac}) can be calculated using the following relation(Dielectrical properties and conduction mechanism of quinoline Schiff base and its complexes n.d.):

$$\sigma_{ac} = \varepsilon_o \omega \varepsilon_2 \quad (10)$$

where ω is the angular frequency ($\omega=2\pi f$. f is the frequency). The temperature dependence of conductivity can be discrepant by the following archaic relation (Effect of Doping with Nickel Ions on the Electrical Properties of Poly(aniline-co-oanthranilic acid) and Doped Copolymer as Precursor of NiO Nanoparticles. In: Foxit. https://www.foxit.com/pdf-to-word/ n.d.).

$$\sigma_{ac} = \sigma_\circ \exp\left(\frac{-\Delta E_{ac}}{k_B T}\right) \quad (11)$$

where $\sigma_\circ$ is the pre-exponential factor and ΔE is the activation energy for AC conductivity, k_B is Boltzmann's constant, and T is the absolute temperature. The relation between σ_{ac} and 1000/T for different test frequency is presented in Fig.8. It is noticed that σ_{ac} demonstrate semiconductor behavior. The thermal activation ΔE_{ac} can be obtained from the slope of the straight line segments in the low and high temperature regions respectively. Fig.9 (a,b) presents the relation of frequency dependence of $\Delta E_{ac(1)}$ and $\Delta E_{ac(2)}$ for TFC in the temperature rang 303 – 385 K and 385 – 440 K, respectively. The value of ΔE_{dc} can be determined from the relation between Ln σ_{ac} versus 1000/T for f= 0 Hz (see Fig. 8). The values of $\Delta E_{dc(1)}$ and $\Delta E_{dc(2)}$ are found to be 0.0576 and 0.617 eV, respectively. The relatively low values of $\Delta E_{ac(1)}$, suggests that the conduction process of charge carries can be described by hoping mechanism (Effect of Doping with Nickel Ions on the Electrical Properties of Poly(aniline-co-oanthranilic acid) and Doped Copolymer as Precursor of NiO Nanoparticles. In: Foxit. https://www.foxit.com/pdf-to-word/ n.d.). Furthermore, in the higher temperature range, the obtained values of $\Delta E_{ac(2)}$ suggest that the conduction of charge carries can be described by thermal activation process.

The AC conductivity (σ_{ac}) can be described as a function of frequency according to the following relation (Elliott 1987).

$$\sigma_{ac} = A\omega^S \quad (12)$$

where, A is a constant depending on temperature and S is the frequency exponent that its behavior with temperature indicates give information about the most probably conduction mechanism(Dielectrical properties and conduction mechanism of quinoline Schiff base and its complexes n.d.). Fig 10. Presents, Ln σ_{ac} as a function of Ln ω in the temperature range 303 - 443 K for TFC. It is observed that

σ_{ac} increases with the increase of frequency in all the frequency range under test. Also, it is observed that, all carves show two different slopes in the low and high regions of frequency. The value of *S* is directly the slope at the higher frequency region. The value of *S* is obtained and presented as a function of temperature in Fig 11. The value of S show a continuous decrease with the increase of temperature. This behavior confirms that the correlated barrier hoping (CBH) mechanism to be the operating condition mechanism. Similar behavior has been recorded for many organic compounds in which the CBH conduction mechanism were proposed as the operating conduction mechanism (N. A. El-Ghamaz1 and E. n.d.; Yu et al. 2017). In CBH model, σ_{ac} is given by the following relation (Bose and Sarma n.d.; Effect of Doping with Nickel Ions on the Electrical Properties of Poly(aniline-co-oanthranilic acid) and Doped Copolymer as Precursor of NiO Nanoparticles. In: Foxit. https://www.foxit.com/pdf-to-word/ n.d.):

$$\sigma_{ac} = \frac{1}{24}\pi^3 N^2 \varepsilon_1 \varepsilon_0 \omega R_\omega^6 \qquad (13)$$

where N is the density of pairs of sites, and R_ω is the hopping distance which can be deduced at angular frequency ω. R_ω is evaluated as follows (El-Nahass, El-Barry, and Abd el Rahman 2006; Geometrical structures, thermal, optical and electrical properties of azo quinoline derivatives n.d.):

$$R_\omega = \frac{e^2}{\pi\varepsilon_1\varepsilon_0[W_m + kTln(\omega\tau_0)]} \qquad (14)$$

where W_m is the maximum barrier height (the energy required moving the electron from a site to infinity and τ_o is the relaxation time with frequency, the ωR_ω^6 component in the CBH model represents frequency dependency and may be represented in terms of the frequency exponent *S* as shown below:

$$S = 1 - \frac{6k_BT}{W_M - kTln(1/\omega\tau_0)} \qquad (15)$$

Which can be approached to the following relation:

$$S = 1 - \frac{6k_BT}{W_M} \qquad (16)$$

As a consequence, the CBH expects a temperature-dependent exponent, *S*, to reduce when the temperature rises and escalates to unity when the temperature declines to zero kelvin.

The maximum barrier height W_m is determined as 2.49 eV. The values of τ_o, r_m, N, For TFC are determined in different temperature and listed in Table 4.

Conclusion

1,2,9-trimethyl-7*H*-furo[3,2-*f*]chromen-7-one] (TFC) is one of coumarin derivatives that showed good thermal stability from room temperature up to approximately 460 K. It decomposed in one major step with maximum decomposition rate at 581 K. The powder of TFC is polycrystalline and has a monoclinic crystal structure with lattice parameters 13.446 Å, 4.566 Å, 10.557 Å, 90^o , 90.62^o and 90^o for a, b, c, α, β and γ, respectively. The average crystallite size was estimated to be 506 nm. The study of the dielectric modulus proved that TFC exhibits minimum polarization at low frequency. The polarization is enhanced with the more increase of applied test frequency which enables more active molecular dynamics and dipole orientation contributing to the overall dielectric response. In general TFC showed semiconductor behavior in the temperature range 303- 440 K. the investigation of conduction mechanism confirmed that the correlated barrier hoping (CBH) mechanism is the operating conduction mechanism for AC conductivity.

Objectives

Computational methods can be employed to provide valuable molecular information for these coumarin derivatives. Therefore, the principal objective of this work was to investigate the structure, electronic and optical properties of these same derivatives (Lin et al. 2008) in order to establish the relationship between the chemical substitutions and computed molecular properties to aid in the design of materials with potential optoelectronic applications.

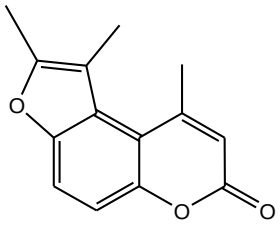

1,2,9-trimethyl-7*H*-furo[3,2-*f*]chromen-7-one(TFC)
Fig.1 The molecular structural for TFC.

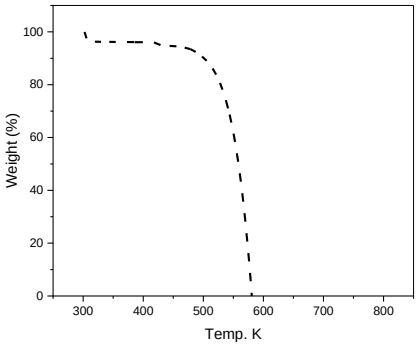

Fig. 2: The TGA curves for TFC.

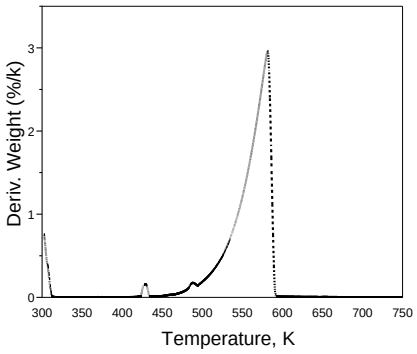

Fig. 3. The DTG curve for TFC.

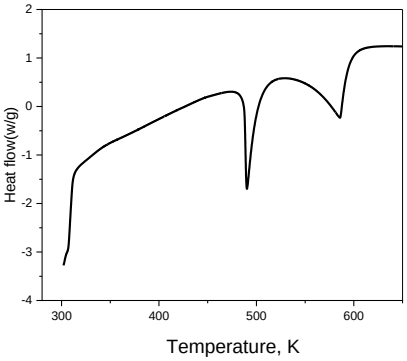

Fig. 4 .The DSC curve for TFC.

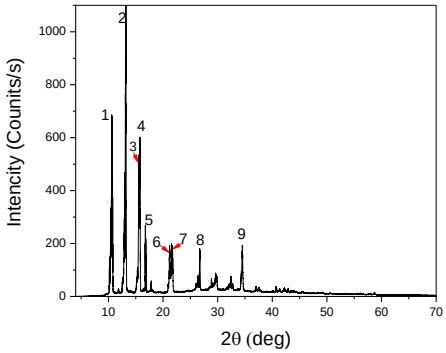

Fig. 5. The XRD patterns for TFC.

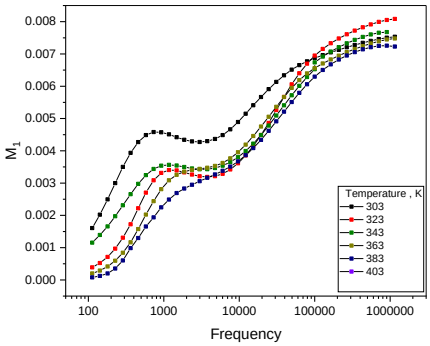

Fig. 6. Frequency dependence of the electric modulus, M_1, for TFC at different temperatures.

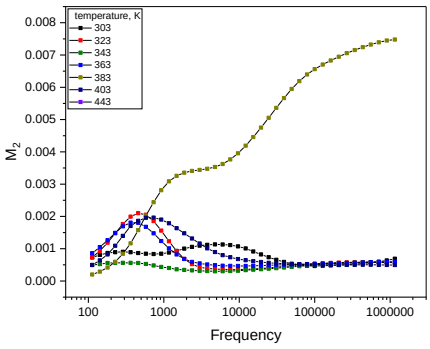

Fig. 7. Frequency dependence of the electric modulus, M_2, for TFC at different temperatures.

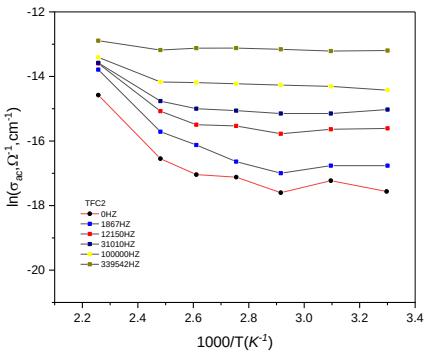

Fig.8. Lnσ_{ac} as a function of 1000/T for TFC.

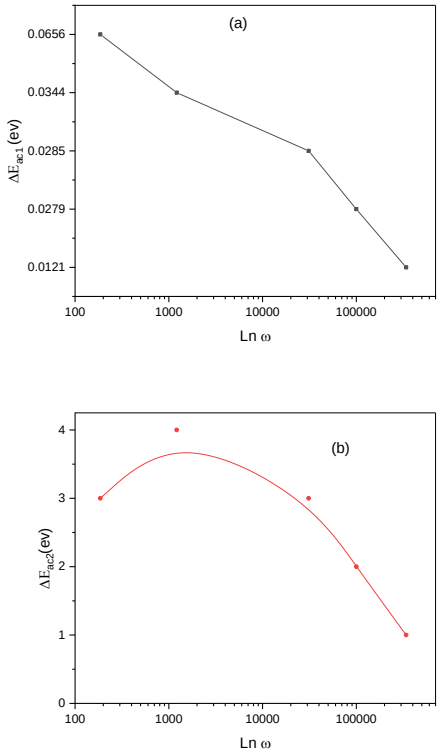

Fig. 9. (a) Temperature dependence of ΔEac_1 and ΔEac_2 respectively
for FTC at different frequencies.

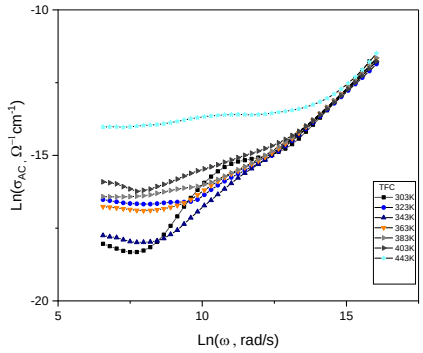

Fig 10. $Ln\sigma_{ac.}$ Versus Lnω for TFC.

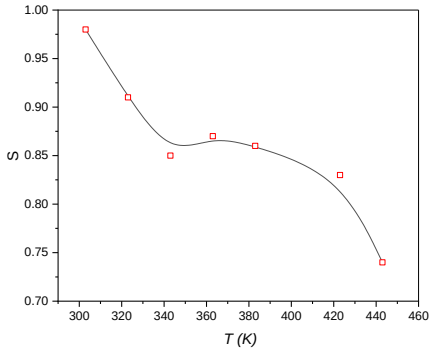

Fig.11**.** the temperature dependence of S for TFC.

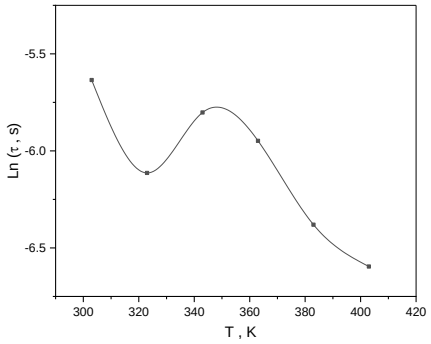

Fig.12 ln (τ,s) as a function of T for TFC.

Table1.The indexed Miller indies (*h k l*) and in inter-planer spacing (d_{hkl}) for TFC.

Selected reflections						
Peak No.	***h k l***	***d hkl***	***2θobs***	***2θcal***	***Δ(2θ)***
1	1 0 1	8.2590	10.6470	10.7024	-0.0554
2	2 0 0	6.7083	13.1591	13.1592	-0.0001
3	$\bar{2}$ 0 1	5.6894	15.5783	15.5378	0.0405
4	2 0 1	5.6370	15.7396	15.6919	0.0477
5	0 0 2	5.2820	16.7894	16.7835	0.0059
6	0 1 1	4.1837	21.2021	21.1833	0.0188
7	3 0 1	4.1034	21.6428	21.6079	0.0349
8	1 1 2	3.3360	26.7225	26.6766	0.0459
9	$\bar{1}$ 0 4	2.5963	34.5080	34.5359	-0.0279

Table 2. The lattice parameters (a, b, c, α, β and γ) and crystal system for TFC.

parameters	**TFC**
Crystal system	Monclinc
a (Å)	13.4460
b (Å)	4.5660
c (Å)	10.5570
α (deg)	90.000
β (deg)	90.62
γ (deg)	90.000
Space group	$P1_2/m$
D (nm)	506.21
δ (m)$^{-2}$x10^{12}	3.9
μ x10^{-3}	0.68

Table 3. The value of *D, δ* and *μ* for TFC.

parameters	TFC
D(nm)	506.21
δ(m)$^{-2}$x10^{12}	3.9
μ x10^{-3}	0.68

Table 4. The W_m is the maximum barrier height, the τ_o is characteristic relaxation time, N expects a temperature-dependent exponent, r_m represents frequency, for TFC.

Compound		**TFC**		***Wm*(eV) = 2.49 eV**
T K	F HZ	τ_o*10^{-3}	r_m×10^{-11}m	N×10^{31}ev/m^3
303	280	3.5714	1.5675	6.3237
323	452	2.2123	1.6648	5.1750
343	331	3.0211	1.5907	6.0459
363	383	2.6109	1.5568	6.5111
383	590	1.6949	1.5139	6.9906
403	732	1.3661	1.4804	7.1834

References

Barot, Kuldipsinh P., Shailesh V. Jain, Laurent Kremer, Shubhra Singh, and Manjunath D. Ghate. 2015. "Recent Advances and Therapeutic Journey of Coumarins: Current Status and Perspectives." *Medicinal Chemistry Research* 24(7): 2771–98. doi:10.1007/s00044-015-1350-8.

Barsoukov, Evgenij, and J. Ross Macdonald. 2005. *Impedance Spectroscopy Theory, Experiment, and Applications.* Hoboken, N.J: Wiley-Interscience.

Bose, K. S., and R. H. Sarma. "Dielectrical Properties and Conduction Mechanism of Quinoline Schiff Base and Its Complexes." *N. A. El-Ghamaz1 • A. A. El-Bindary2 • M. A. Diab2 • A. Z. El-Sonbati2 • S. G. Nozha2* 66(4). doi:10.1007/s11164-015-2164-5.

"Conducting Polymers. VII. Effect of Doping with Iodine on the Dielectrical and Electrical Conduction Properties of Polyaniline." *Foxit*. www.tandfonline.com/lsrt. (September 2, 2024).

"Correlation between Ionic Radii of Metal Azodye Complexes and Electrical Conductivity." *Foxit*. m.adiab@yahoo.com (M.A. Diab).

Detsi, Anastasia, Christos Kontogiorgis, and Dimitra Hadjipavlou-Litina. 2017. "Coumarin Derivatives: An Updated Patent Review (2015-2016)." *Expert Opinion on Therapeutic Patents* 27(11): 1201–26. doi:10.1080/13543776.2017.1360284.

"Dielectrical Properties and Conduction Mechanism of Quinoline Schiff Base and Its Complexes." *Foxit*. A. Z. El-Sonbati elsonbatisch@yahoo.com (September 2, 2024).

Dinnebier, R. "From the Editor of Newsletter 32."

Effect of Doping with Nickel Ions on the Electrical Properties of Poly(aniline-co-oanthranilic acid) and Doped Copolymer as Precursor of NiO Nanoparticles. In: Foxit. https://www.foxit.com/pdf-to-word/. "Effect of Doping with Nickel Ions on the Electrical Properties of Poly(Aniline-Co-Oanthranilic Acid) and Doped Copolymer as Precursor of NiO Nanoparticles. In: Foxit. Https://Www.Foxit.Com/Pdf-to-Word/." Effect of Doping with Nickel Ions on the Electrical Properties of Poly(aniline-co-oanthranilic acid) and Doped Copolymer as Precursor of NiO Nanoparticles. In: Foxit. https://www.foxit.com/pdf-to-word/.

El-Ghamaz, N. A., M. S. Moqbel, and M. M. El-Shabaan. 2020. "Theoretical and Experimental Studies on Structural and Optical Properties of Two Quinoxaline 1,4dioxide Derivatives." *Journal of Materials Science: Materials in Electronics* 31(24): 22012–27. doi:10.1007/s10854-020-04703-x.

Elgogary, Sameh Ramadan, Neveen Mohamed Hashem, and Mohamed Nabeel Khodeir. 2015. "Synthesis and Photooxygenation of Linear and Angular Furocoumarin Derivatives as a Hydroxyl Radical Source: Psoralen, Pseudopsoralen, Isopseudopsoralen, and Allopsoralen." *Journal of Heterocyclic Chemistry* 52(2): 506–12. doi:10.1002/jhet.2084.

Elliott, S.R. 1987. "STUDY THE ELECTRICAL PROPERTIES AND AC CONDUCTIVITY OF OURE PMMA AND PMMA DOPED WITH AZO DYE." *International Journal of Physics* 36(2): 135–217. doi:editor@tjprc.org.

El-Nahass, M. M., A. A. Atta, H. E. A. El-Sayed, and E. F. M. El-Zaidia. 2008. "Investigations on Growth, XRD, Strain, FTIR, UV–Vis NIR, Photoluminescence, SHG, and Z-Scan Analyses of L-Cysteine Picrate Single Crystal for NLO and Optical Limiting Applications." *Applied Surface Science* 254(8): 2458–65.

El-Nahass, M. M., A. M. A. El-Barry, and S. Abd el Rahman. 2006. "Ac Conductivity and Dielectric Properties of TlIn 0.975 Y 0.025 S 2 Single Crystal." *physica status solidi (a)* 203(2): 317–26. doi:10.1002/pssa.200521304.

El-Nahass, M.M., and H.A.M. Ali. 2012. "AC Conductivity and Dielectric Behavior of Bulk Furfurylidenemalononitrile." *Solid State Communications* 152(12): 1084–88. doi:10.1016/j.ssc.2012.03.002.

"Geometrical Structures, Thermal, Optical and Electrical Properties of Azo Quinoline Derivatives." *Foxit*. www.elsevier.com/locate/molliq.

Goel, Atul, Vijay Kumar, Salil P. Singh, Ashutosh Sharma, Sattey Prakash, Charan Singh, and R. S. Anand. 2012. "Non-Aggregating Solvatochromic Bipolar Benzo[f]Quinolines and Benzo[a]Acridines for Organic Electronics." *Journal of Materials Chemistry* 22(30): 14880–88. doi:10.1039/C2JM31052J.

Jonscher, Andrew K. 1999. "Dielectric Relaxation in Solids." *Journal of Physics D: Applied Physics* 32(14): R57–70. doi:10.1088/0022-3727/32/14/201.

Jung, Woo-Hwan. 2013. "Dielectric Relaxation and Hopping Conduction in La 2 NiO 4+ δ." *Journal of Materials* 2013: 1–6. doi:10.1155/2013/169528.

Kadhum, Abdul Amir H., Ahmed A. Al-Amiery, Ahmed Y. Musa, and Abu Bakar Mohamad. 2011. "The Antioxidant Activity of New Coumarin Derivatives." *International Journal of Molecular Sciences* 12(9): 5747–61. doi:10.3390/ijms12095747.

Kotchapadist, Palita, Narid Prachumrak, Thitiya Sunonnam, Supawadee Namuangruk, Taweesak

Sudyoadsuk, Tinnagon Keawin, Siriporn Jungsuttiwong, and Vinich Promarak. 2015. "Synthesis, Characterisation, and Electroluminescence Properties of N-Coumarin Derivatives Containing Peripheral Triphenylamine." *European Journal of Organic Chemistry* 2015(3): 496–505. doi:10.1002/ejoc.201402680.

Kumar, Shiv, Boregowda Puttaraju, and Satish Patil. 2016. "A Deep-Blue Electroluminescent Device Based on a Coumarin Derivative." *ChemPlusChem* 81(4): 384–90. doi:10.1002/cplu.201500572.

Lin, Hsiu-Chen, Shin-Hui Tsai, Chien-Shu Chen, Yuan-Ching Chang, Chi-Ming Lee, Zhi-Yang Lai, and Chun-Mao Lin. 2008. "Powder3D: An Easy to Use Program for Data Reduction and Graphical Presentation of Large Numbers of Powder Diffraction Patterns." *Biochemical Pharmacology* 75(6): 1416–25. doi:10.1016/j.bcp.2007.11.023.

Liu, Xiaogang, Jacqueline M. Cole, and Kian Sing Low. 2013. "Conducting Polymers. VI. Effect of Doping with Iodine on the Dielectrical and Electrical Conduction Properties of Polyacrylonitrile." *The Journal of Physical Chemistry C* 117(28): 14731–41. doi:10.1021/jp310397z.

Mohammed, Ali Y., and Luma S. Ahamed. 2022. "Synthesis and Characterization of New Substituted Coumarin Derivatives and Study Their Biological Activity." *Chemical Methodologies* (Online First). doi:10.22034/CHEMM.2022.349124.1569.

N. A. El-Ghamaz1 and E., Hajer Abusnina. *AC Electrical Properties, Thermal Analysis and Emission Spectrum of Chitosan Polymer*.

P, Jigar L. *The Introduction of Coumarin*. Blue Rose Publishers.

Pedro, Gonçalo, Frederico Duarte, Dmitrii A. Cheptsov, Nikita Yu Volodin, Ivan V. Ivanov, Hugo M. Santos, Jose Luis Capelo-Martinez, et al. 2023. "Exploring Coumarin-Based Boron Emissive Complexes as Temperature Thermometers in Polymer-Supported Materials." *Sensors* 23(3): 1689. doi:10.3390/s23031689.

Pramod, A. G., C. G. Renuka, and Y. F. Nadaf. 2019. "Electronic Structure, Optical Properties and Quantum Chemical Investigation on Synthesized Coumarin Derivative in Liquid Media for Optoelectronic Devices." *Journal of Fluorescence* 29(4): 953–68. doi:10.1007/s10895-019-02409-w.

Sarker, Satyajit D., and Lutfun Nahar. 2017. "Progress in the Chemistry of Naturally Occurring Coumarins." In *Progress in the Chemistry of Organic Natural Products 106*, eds. A. Douglas Kinghorn, Heinz Falk, Simon Gibbons, and Jun'ichi Kobayashi. Cham: Springer International Publishing, 241–304. doi:10.1007/978-3-319-59542-9_3.

Satyanarayana, V. S. V., P. Sreevani, Amaravadi Sivakumar, and V. Vijayakumar. 2009. "Synthesis and Antimicrobial Activity of New Schiff Bases Containing Coumarin Moiety and Their Spectral Characterization." *Arkivoc* 2008(17): 221–33. doi:10.3998/ark.5550190.0009.h21.

Sontisiri, Pakornsiri, Dusit Promrug, Dumrongkiet Arthan, Nathawut Choengchan, and Panumart Thongyoo. 2025. "A New Coumarin-Based 'OFF–ON' Fluorescent Sensor for H2S Detection in HeLa Cells." *Spectrochimica Acta Part A: Molecular and Biomolecular Spectroscopy* 326: 125170. doi:10.1016/j.saa.2024.125170.

Sun, Xiao-ya, Teng Liu, Jie Sun, and Xiao-jing Wang. 2020. "Synthesis and Application of Coumarin Fluorescence Probes." *RSC Advances* 10(18): 10826–47. doi:10.1039/C9RA10290F.

Tan, K B, and H Shaari. 2008. "Reaction Study and Phase Formation in Bi 2O3-ZnO-Nb 2O5 Ternary System." . *Number* 9(2).

Xu, Zhi, Qingtai Chen, Yan Zhang, and Changli Liang. 2021. "Electronic Conduction Mechanism and Optical Spectroscopy of Indigo Carmine as Novel Organic Semiconductors." *Fitoterapia* 150: 104863. doi:10.1016/j.fitote.2021.104863.

Yu, Tianzhi, Zeyang Zhu, Yanjun Bao, Yuling Zhao, Xiaoxiao Liu, and Hui Zhang. 2017. "AC Conductivity and Dielectric Behavior of Bulk Furfurylidenemalononitrile." *Dyes and Pigments* 147: 260–69. doi:10.1016/j.dyepig.2017.08.017.

الملخص العربي

عنوان البحث: دراسة الخصائص التركيبية و الحرارية و خواص العزل الكهربى لمشتق الكومارين (CFT) -1,2,9 trimethyl-7H-furo[3,2-f]chromen-7-one]

عفاف ميلاد على*[١]، ناصر عبده عبد الرزاق الغماز[١]، مي محمود محمد الشبعان[١]

[١] قسم الفيزياء ـ كلية العلوم ـجامعة دمياط ـ دمياط ـ مصر

فى الدراسة الحالية تمت دراسة الخواص التركيبية و الحرارية و خواص العزل الكهربى لأحد مشتقات الكومارين (CFT) .
أظهرت الدراسة أن CFT ذات طبيعة عديدة التبلور حيث أن بلوراتة لها شكل أحادى الميل وتم قياس متوسط حجم البلورة فكان ٥٠٦ نانو متر .
أظهرت دراسة معامل العزل الكهربي (suludom cirtceleid) أن مشتقة الكومارين CFT لها معامل استقطاب صغير جدا عند الترددات المنخفضة و مع زيادة التردد يتحسن معامل ألاستقطاب مما يسهل ديناميكية الجزيئات و تحسن الاستجابة للمجال الكهربى المتردد.
وجد أن CFT يظهر سلوك أشباه الموصلات ووجد أن ألية التوصيل للتيار المتردد هى ألية القفز المترابط عبر حواجز الطاقة (HBC).